HHS Public Access

Author manuscript

ACS Appl Mater Interfaces. Author manuscript; available in PMC 2024 January 13.

Published in final edited form as:

ACS Appl Mater Interfaces. 2023 July 12; 15(27): 32188–32200. doi:10.1021/acsami.3c03528.

β-Glucan-Mediated Oral Codelivery of 5FU and Bcl2 siRNA Attenuates Stomach Cancer

Humayra Afrin,
Environmental Science & Engineering, University of Texas at El Paso, El Paso, Texas 79965, United States; Department of Pharmaceutical Sciences, School of Pharmacy, University of Texas at El Paso, El Paso, Texas 79902, United States

Stephanie Vargas Esquivel,
Department of Pharmaceutical Sciences, School of Pharmacy, University of Texas at El Paso, El Paso, Texas 79902, United States; Department of Aerospace & Mechanical Engineering, College of Engineering, University of Texas at El Paso, El Paso, Texas 79965, United States

Raj Kumar,
Department of Pharmaceutical Sciences, School of Pharmacy, University of Texas at El Paso, El Paso, Texas 79902, United States; Biomedical Engineering, College of Engineering and Department of Industrial, Manufacturing and Systems Engineering, University of Texas at El Paso, El Paso, Texas 79965, United States

Md Ikhtiar Zahid,
Environmental Science & Engineering, University of Texas at El Paso, El Paso, Texas 79965, United States; Department of Pharmaceutical Sciences, School of Pharmacy, University of Texas at El Paso, El Paso, Texas 79902, United States

Beu Oporeza,
Biomedical Engineering, College of Engineering, University of Texas at El Paso, El Paso, Texas 79965, United States

Md Fashiar Rahman,
Department of Industrial, Manufacturing and Systems Engineering, University of Texas at El Paso, El Paso, Texas 79965, United States

Corresponding Author: **Md Nurunnabi** – Environmental Science & Engineering and Biomedical Engineering, College of Engineering, University of Texas at El Paso, El Paso, Texas 79965, United States; Department of Pharmaceutical Sciences, School of Pharmacy, University of Texas at El Paso, El Paso, Texas 79902, United States; Border Biomedical Research Center, University of Texas at El Paso, El Paso, Texas 79965, United States; Phone: 915-757-8335; mnurunnabi@utep.edu.

Author Contributions

H.A. and M.N. designed and prepared the methodology for the experiment. H.A., B.O., S.V.E., M.I.Z., and R.K. conducted the experiment. M.F.R. conducted the image analysis. H.A. and M.N. prepared the manuscript. All the authors revised and approved the manuscript.

Supporting Information

The Supporting Information is available free of charge at https://pubs.acs.org/doi/10.1021/acsami.3c03528.

Formulation stability data, additional SEM images for BG/FU and BG/siRNA, drug release profile, siRNA stability by western blotting, SPR spectrum, in vitro cytotoxicity data, graphical images of intestines, and additional H&E images of the duodenum, jejunum, and ileum (PDF)

Complete contact information is available at: https://pubs.acs.org/10.1021/acsami.3c03528

The authors declare the following competing financial interest(s): Md Nurunnabi serves as Scientific Advisory board for KB BioMed Inc and Filament LLC (Dunatech) and owns equity for Dunatech LLC. Md Nurunnabi, Humayra Afrin and Raj Kumar are an inventor on patents related to the tools and methods reported in this manuscript (owned and managed by University of Texas at El Paso).

Thomas Boland,
Biomedical Engineering, College of Engineering, University of Texas at El Paso, El Paso, Texas 79965, United States

Md Nurunnabi
Environmental Science & Engineering, University of Texas at El Paso, El Paso, Texas 79965, United States; Department of Pharmaceutical Sciences, School of Pharmacy, University of Texas at El Paso, El Paso, Texas 79902, United States

Abstract

Based on cancer-related deaths, stomach cancer is ranked fifth, and first among Hispanics. Lack of technologies for early diagnosis and unavailability of target-specific therapeutics are largely the causes of the poor therapeutic outcomes from existing chemotherapeutics. Currently available therapeutic modalities are invasive and require systemic delivery, although the cancer is localized in the stomach at its early stage. Therefore, we hypothesize that an oral local delivery approach can extend the retention duration of the therapeutics modalities within the stomach and thereby enhance therapeutic efficacy. To accomplish this, we have developed a ß-glucan (BG)-based oral delivery vehicle that can adhere to the mucus lining of the stomach for an extended period while controlling the release of Bcl2 siRNA and 5-fluorouracil (5FU) payload for over 6 h. We found that Bcl2 siRNA selectively knocked down the Bcl2 gene in a C57BL/6 stomach cancer mouse model followed by upregulation of apoptosis and remission of cancer. BG was found to be very effective in maintaining the stability of siRNA for at least 6 h, when submerged in simulated gastric juice tested in vitro. To investigate the potential therapeutic effects in vivo, we used a stomach cancer mouse model, where C57BL/6 mice were treated with 5FU, BG/5FU, siRNA, BG/siRNA, and BG/5FU/siRNA. Higher inhibition of Bcl2 and therapeutic efficacy were observed in mice treated with BG/5FU/siRNA confirmed with Western blotting and a TUNEL assay. Significant reduction in the tumor region was observed with histology (H&E) and immunohistochemistry (Ki67, TUNEL, and Bcl2) analyses. Overall, the oral formulation shows improved efficacy with nonsignificant side effects compared to the conventional treatment tested in the gastric cancer mouse model.

Graphical Abstract

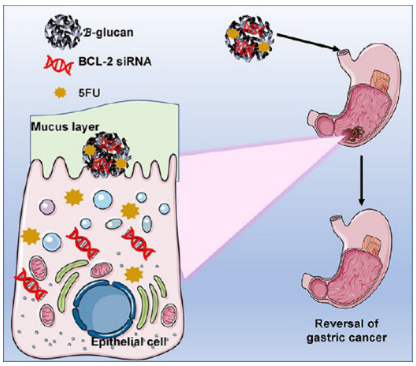

Keywords

stomach cancer; oral biologics; oral local delivery; stomach specific

1. INTRODUCTION

Stomach cancer is the fifth most common cancer by incidence and the third most deadly cancer.[1] In 2018, 782,685 out of 1,033,701 patients died of stomach cancer worldwide.[2] According to data from the American Cancer Society, 26,380 new stomach cancer patients were diagnosed solely in the United States in 2022, and among the diagnosed individuals, 11,090 died. Currently available therapeutic interventions for stomach cancer treatment are chemotherapy, immunotherapy, radiotherapy, and surgery. Among FDA-approved chemotherapeutic drugs, 5-fluorouracil (5FU), capecitabine, docetaxel, epirubicin, doxorubicin, trastuzumab, trifluridine, and tipiracil are most widely considered in clinic for stomach cancer treatment.[3] Other promising drugs are those developed for immunotherapy, such as PDL1 inhibitors like pembrolizumab or nivolumab, and targeted gene therapy drugs have also shown promise for stomach cancer therapy.[4] Some genes (for instance, IL-8, CLDN1, KRT17, CLDN7, and MMP7) are reportedly upregulated and some other genes (for instance, GAS5, ZIC1, RASAL1, *GPER*, *KIAA1324*, *ADA*, and *SLC9A2*) are found to be downregulated in stomach cancer.[5–8] It has also been reported that upregulation of STAB1, STAT3, Bcl2, and Bcl-xL genes occurs in the stomach during the cancerous state.[8,9]

Like the treatment of other cancers, for stomach cancer treatment, dosage form, route of administration, and dosage amount of the chemotherapeutics are crucial to avoiding potential severe risks of toxicity to the healthy tissue associated with nonspecific distribution. Stomach cancer management is severely challenging due to the difficulty to deliver the appropriate amount of drug to the location of the cancer and maintain its therapeutic concentration for a prolonged duration, regardless of the route of administration. This is further compounded by the relatively late diagnosis that is more typical of stomach cancer patients and that occurs when the cancer has grown and spread across the stomach.[10] In addition, oral administration of the chemotherapeutics is not very effective due to the bowel movement and shorter retention duration. The retention duration of any orally administered drug to the stomach is 10–30 min, much less than the duration often needed to induce an adequate therapeutic effect and maintain the appropriate therapeutic concentration within the cancer site.[11,12] Finally, oral delivery of therapeutic modalities is challenging because of the significantly low bioavailability resulting from poor intestinal permeability, enzymatic degradation, thick mucus membrane barrier, and off-target localization.[13] In order to overcome these issues, we aim to develop an oral local delivery vehicle, made from the mucoadhesive carrier b-glucan (BG).[14] BG is a unique carbohydrate polymer that is naturally present in the cell wall of yeast, fungi, and cereal. BG used in this study is a barley-derived low-viscosity glucose polymer with a molecular weight of 179,000 Da. We have previously reported that BG is very stable in acidic buffer, has a strong binding affinity with mucin, and forms microstructure particles in the presence of fatty acids.[14] Studies show that the BG-based vehicle is highly effective in oral vaccine and protein delivery.[15,16] The BG-mediated mucoadhesive particle has the ability to protect therapeutic regimens

from the harsh gastric environment, enhance retention of the therapeutic payload within the stomach for a longer duration, and maintain a sufficient therapeutic concentration for a prolonged period (6 h or more).[17] In addition, BG was found to act as an immune modulator of the gastrointestinal (GI) tract.[18] Finally, BG has also shown significant potential in GI site-specific drug delivery to treat liver diseases, bowel disease, and stomach cancer.[17,19–21]

5FU is a pyrimidine analog, a potent and widely used chemotherapy to treat GI-tract-related cancers including stomach cancer.[22,23] A meta-analysis of stomach cancer treatment revealed a significant advantage in terms of 3-year survival when on chemotherapy with S-1, an oral 5FU derivative (80%), compared to surgery (70%). 5FU or S-1 is considered as first-line treatment due to its better efficacy but is recommended to be administered with adequate precaution to avoid the severe risk of side effects associated with toxicity.[24] Despite having higher therapeutic effectivity, oral delivery causes various side effects within the GI tract and intravenous administration produces toxicities in major organs including the heart, lungs, and kidney.[25] Side effects of 5FU include cardiotoxicity, hypotension, breathing problem, hair loss, and weight loss.[25] With the development of a delivery platform that has the potential to minimize systemic distribution of 5FU and increase the drug concentration within the site of cancer, it is highly likely possible to minimize drug-mediated toxicity and increase therapeutic effects. Besides, 5FU itself is not very effective for treating cancer; for instance, the treatment response rate is between 10 and 15% for advanced colorectal cancer. Therefore, we presume that a combination of RNAi can improve the therapeutic effect by synergizing the mechanism of action. Therefore, we aim to incorporate a Bcl2 small interfering RNA (siRNA) that holds emerging promise for the genetic treatment of cancer. Since its discovery, siRNA has been considered to be applied as gene therapy for treatments of various cancers including stomach cancer.[26,27]

Bcl2 overexpression has been found in cancers including the stomach, breast, and pancreas, where it promotes the proliferation of cancer cells.[28–31] Bcl2 downregulation has also been reported to induce apoptosis to tumor cells and make them more sensitive to chemotherapy.[32] Some recent reports have demonstrated strategies for improved oral delivery of siRNA to ameliorate hepatic cancer through nanoparticles and mucoadhesive molecules.[33] The Bcl2 family is composed of a subset of proteins that act as apoptosis regulators. Research suggested that the hyperactivation of Bcl2-related anti-apoptotic effects correlates with cancer occurrence, progression, and prognosis. Therefore, we hypothesize that a combination of Bcl2 siRNA and 5FU can accelerate stomach cancer therapeutic outcomes when given orally (Scheme 1).

To prove the concept and to investigate therapeutic feasibility, 5FU and siRNA were loaded within a nanoparticle composed of BG. Both physical and chemical characterizations were conducted prior to utilizing the formulation for in vitro and in vivo studies. We have observed that BG-based oral vehicles not only increase retention of the payload of 5FU and siRNA within the stomach but also facilitate sustained release of the payload for over 6 h. In vivo studies revealed that the oral delivery of BG/siRNA/5FU downregulates the Bcl2 protein by 60% and increases apoptosis by 140% with a daily oral dose for 15 days. Immunohistochemistry analysis of stomach tissue also shows that Ki67 expression reduces by 300% compared to untreated cancer and 5FU groups and 200% compared

to the siRNA-treated group. These results are an obvious indication of the potency and effectiveness of the BG-based oral formulation of siRNA/5FU. Toxicological studies including histochemistry and serum biochemistry also demonstrate the biosafety of the orally administered siRNA/5FU formulation and hold a strong promise for pre-clinical studies with larger animals.

2. MATERIALS AND METHODOLOGY

2.1. Materials.

The human colon cancer cell line (CaCo2) and stomach cancer cell line (AGS) were purchased from ATCC (Manassas, Virginia). 5FU, sodium dodecyl sulfate, and Coumarin 6 were purchased from Sigma-Aldrich (St. Luis, Missouri). β-Glucan (MW 179,000) was purchased from Megazyme (Wicklow, Ireland). Bcl2 siRNA was purchased from Cell Signaling Technology (Danvers, Massachusetts). Fetal bovine serum (FBS), penicillin, phosphate-buffered saline (PBS), and 0.05% Trypsin–EDTA were purchased from Life Technologies (Carlsbad, CA). Bcl-2 SiRNA I (Cat #6441) was purchased from Cell Signaling Technology (Danvers, MA). Bcl2 antibody, Ki-67 antibody, and FITC-Goat anti-Rabbit IgG were purchased from ABclonal (Woburn, Massachusetts). Simulated gastric juice was purchased from RICCA (Arlington, Texas). Click-iT Plus TUNEL assay, eosin, xylene, Harris hematoxylin, was purchased from Fisher Scientific (Waltham, Massachusetts).

2.2. Preparation of BG and Formulations.

BG NPs were prepared by the direct physical mixing method. In details, 30 mg of BG was dissolved in 1 mL of DI water upon heating at 80 °C and constant stirring for 15–20 min. Upon heating and continuous stirring, BG formed a transparent gel-like solution. Thereafter, with heating discontinued, 12 mg of 5FU was directly added to the BG solution and kept stirred for an additional 30 min for uniform mixing.

To prepare BG/5FU/siRNA, 12 μL of siRNA was added in BG/5FU under constant stirring. Then, it was mixed with alternate sonication and vortexing. The siRNA-loaded BG nanoparticle was prepared via electrostatic interaction. 30 mg of BG was dissolved in 1 mL of DI water upon heating at 80 °C and constant stirring for 15–20 min. 12 μL (12 nM) of siRNA was added into the BG solution at room temperature. The siRNA solution was added to the BG solution dropwise under vigorous stirring for 10 min. The BG/siRNA nanoparticles formed via electrostatic interaction between BG and siRNA.

2.3. Characterization of the Formulations.

The particle size and zeta potential of BG formulations were determined by a Zetasizer (Nano ZS, Malvern Instruments, Worcestershire, UK) and kept at 25 °C during the measuring process. All formulations were analyzed three times, and the results are presented as the mean. The stability of the formulations and their individual payload were evaluated in saline (pH 7.4) and simulated gastric juice (pH 1–1.4) at different time points. For measuring the size and zeta potential of BG, BG/5FU, BG/siRNA, and BG/5FU/siRNA, all the formulations were diluted in deionized water.

2.4. In Vitro Release Study.

In vitro release was studied using a dialysis bag against simulated gastric juice. Briefly, free 5FU, BG/5FU, and BG/5FU/siRNA were taken into the dialysis bag individually. 2 mg of 5FU was dissolved in 100 μL of DMSO and dialyzed against 50 mL of simulated gastric juice (pH 1–1.4, 37 °C) with 2 kDa MWCO dialysis bags and continuous stirring at 100 RPM. 1 mL of solution was collected from the outer phase every 2 h for a 12 h, period and the same volume of GJ was added to maintain the volume. The release amount of 5FU into the GJ was quantified by measuring the absorbance at the wavelength of 265 nm by a UV–visible spectrophotometer (UV-2800, Shimadzu spectrophotometer).[34]

2.5. Stability of the Formulation.

To examine the stability of the formulations, naked siRNA and siRNA with BG were diluted in PBS and incubated with BG at 37 °C for 0, 1, 2, 4, and 6 h and the size and zeta potential were measured. To measure the stability of siRNA in gastric juice with and without BG, siRNA and BG/siRNA were diluted with simulated gastric juice and incubated for 0, 1, 2, 4, and 6 h and then the size and zeta potential were measured according to the method demonstrated earlier. Gel electrophoresis of these formulations was also conducted to confirm the stability of loaded siRNA. To determine the stability of siRNA within BG, the siRNA samples were separated into 1% agarose gels. Agarose solution was prepared by dissolving in 1× TAE and heated in a microwave for 3 min until dissolved completely. Ethidium bromide was added to the solution before pouring the agarose solution into the casting stand, and a 10-well comb was placed to generate wells that are 1.5 mm deep. The melted agarose was allowed to cool for 30 min at room temperature for polymerization. The chamber was filled with 1× TAE buffer solution to a height of 1.5 cm above the gel surface. RNA samples were premixed with the agarose gel loading dye (6×) prior to loading 20 μL (1 μL siRNA, 3 μL dye with 6 μL of simulated gastric juice, and 10 μL BG) of samples into the wells from left to right. The power supply was activated as soon as all wells were filled, to avoid initial diffusion of the dye into the gel. The samples were run at 100 V for 40 min and were imaged using ChemiDoc imaging system (Bio-Rad, USA). The formulations were incubated in GJ for 0, 1, 2, 4, 6, and 8 h prior to measurement of the stability of the payload of siRNA. The stability of naked siRNA and BG/siRNA in GJ was also measured by the NanoDrop as well.

2.6. Ex Vivo Diffusion Study.

To measure the diffusion of hydrophobic small molecules through the intestinal layer, an ex vivo study with the porcine intestine was done. Here, coumarin 6 was used as a model hydrophobic molecule instead of 5FU for visualization purposes. Coumarin 6 and BG/coumarin 6 was added over the porcine intestine for different time points. In each time point, the intestine was washed with PBS for 5 min and then subjected to imaging. The BG/coumarin 6 particle was prepared by O/W emulsion.

2.7. Surface Plasmon Resonance (SPR) to Demonstrate the Binding Interaction between Formulations and Mucin.

To demonstrate the physical and chemical interactions between the BG-based formulations and mucin, we used the SPR (ibClu, South Korea) technique. The BG solution was run over a carboxylate-functionalized (−COOH) Au chip, 1× PBS was used as a running buffer, and 50 μM mucin was used as an analyte. The experiment was conducted according to the manufacturer's instruction. Briefly, EDC and NHS were added over the COOH-Au chip for 3 min with real-time monitoring. Then, BG was run over the chip for 5 min at a flow rate of 30 μL/min followed by running of ethanolamine blocking buffer. From the change of response from the baseline, immobilization of BG was confirmed. After immobilizing the chip with BG, mucin was injected at a flow rate of 30 μL/min for 5 min and after that a regeneration buffer was injected to wash out the excess analyte from the chip. The data was collected from the software and graphs were plotted in Prism GraphPad.

2.8. Cell Culture.

For the cell experiment, AGS cell lines were used. The cells were cultured at 37 °C in a humidified atmosphere containing 5% CO_2 in DMEM supplemented with 10% FBS. 5000 cells per well were seeded in a 96-well plate and incubated overnight. BG formulations with different concentrations of 5FU (45, 35, 25, 15, and 5 μM), and 1 nM of siRNA were added into the cells and incubated for 24 h. To measure cytotoxicity, an MTT assay kit (Vybrant MTT Cell Proliferation Assay Kit, Thermo Fisher) was used according to the manufacturer's instructions. In brief, 10 μL of the MTT solution was mixed with 100 μL of the culture medium for 4 h in the incubator. Then, 100 μL of SDS–HCl solution was added to each well and mixed well. Then, incubated for another 12 h in a humidified chamber. Finally, the absorbance at 570 nm was taken. Healthy cells without any formulation were used as a control; background absorbance was subtracted from each value, and the cell viability percentage was measured.[35] The data is provided in Supplementary Figure S7.

2.9. Development of the Stomach Cancer Mouse Model.

All animal experiments were carried out in strict accordance with protocols approved by the Animal Care and Use Committee of the University of Texas at El Paso and comply with the National Research Council's Guide for the Care and Use of Laboratory Animals. Both male and female (50:50) mice were chosen for the experiments, as sex has no significant influence in stomach cancer. A stomach cancer mouse model was developed by feeding *N*-methyl-*N*-nitrosourea (NMNU) with water (IACUC protocol no. A-201019-A). The 6-week-old C57BL/6 mice were kept in a 12 h light–12 h dark cycle. The mice had unprotected access to food and water. NMNU was dissolved in distilled water available ad libitum, freshly prepared three times per week. The mice received 240 ppm NMNU in the drinking water over 5 weeks (every other week). Five weeks after NMNU administration, the mice were ready for the experiment, as in the method reported elsewhere.[36,37] A total of 30 stomach cancer mice were prepared and divided randomly into five groups—no treatment (control), 5FU, BG/5FU, siRNA, BG/siRNA, and BG/5FU/siRNA. Another group of healthy mice were used as a negative control without any treatment. To investigate therapeutic feasibility, 5FU (10 mg/kg) and siRNA (100 nM) were administered either orally (PO) or intravenously

(IV). All the formulations were freshly prepared prior to administration. Formulations were administered orally on every third day for the subsequent five cycles over 15 days. The animals were sacrificed 72 h after the last treatment followed by the organ harvest and blood collection for further studies. Immediately after harvesting, the size and weight of the stomach and intestine were measured.

2.10. In Vivo and Ex Vivo Imaging for Biodistribution.

To understand the absorption and biodistribution profile of the orally administered formulation, coumarin 6, a fluorescent dye was loaded with BG and orally administered via gavage to mice. For in vivo imaging, the mice were anesthetized and then imaged using an in vivo imaging system (IVIS) at different time points of post-administration, according to the method published earlier.[38] For the ex vivo imaging, the mice were sacrificed after 2, 4, and 6 h of post-administration, and the organs were harvested, followed by imaging using the IVIS.

2.11. In Vivo Protein Expression.

The fresh frozen stomach tissue was homogenized using RIPA buffer with a freshly prepared protease inhibitor in it. The homogenate was then centrifuged at 13,000 rpm for 10 min at 4 °C. The supernatant was collected, and the total protein content was determined using Bradford's assay (Sigma-Aldrich). SDS-PAGE (12%) was performed to separate protein samples (30 μg) at 70–80 V for 3 h at room temperature. Later, the proteins were transferred to a PVDF membrane using a transfer unit run at 25 V overnight at 4 °C. The PVDF membrane was blocked by incubating with 3% BSA containing TBST for 90 min. The membrane was incubated with Bcl2 and β-actin primary antibodies (ABclonal, USA) overnight at 4 °C. After three washing cycles with ice-cold PBS, the membrane was incubated with a horseradish peroxidase-conjugated secondary antibody (ABclonal, USA) for 2 h at room temperature. The primary and secondary antibodies were used at a 1:1000 dilution ratio. The membrane was treated with an ECL mixture. The bands were visualized using a ChemiDoc imaging system (Bio-Rad, USA). The band intensities were calculated using ImageJ software.

2.12. Histology.

Three days after the last treatment, the animals were sacrificed to harvest the organs for further histology and immunohistochemistry. Different parts of the intestine (duodenum, jejunum, and ileum) were embedded in OTC, and the other organs were embedded in paraffin. Fresh frozen stomach was processed in an STP 120 Spin Tissue Processor (Fisher Scientific, USA) and embedded in paraffin on the following day. The tissue was cut at 6 μm thickness and was attached on a Superfrost Plus slide (Fisher Scientific, USA). The slides with tissue sections were used for H&E staining, immunofluorescence assay, and TUNEL assay. H&E images were taken using a MoticEasyScan One slide scanner (Motic Digital Pathology, USA) and a Leica DM 6000B fluorescent microscope.

2.13. Immunofluorescence and Immunohistochemistry Analysis.

Immunofluorescence analysis was performed to understand the Bcl2 and Ki67 protein expression in tumor tissues after treatment with different formulations. The 6 μm-thin sections were obtained by sectioning paraffin-embedded colon tissues using a microtome. Sections were mounted onto poly-L-lysine-coated Superfrost Plus charged glass slides and rehydrated in multiple concentrations of alcohol and xylene for 5 min each. Sections were incubated with antigen retrieval sodium citrate buffer (10 mM sodium citrate buffer pH 6, 0.05% Tween 20) at 90–95 °C for 10 min and blocked using 2.5% bovine serum albumin (BSA) in Tris-buffered saline for 1 h at room temperature. Then, the sections were incubated with Bcl2 and Ki67 primary antibodies (at 1:100 and 1:50 dilution ratios) overnight at 4 °C. The next day, the sections were incubated with FITC-Goat Anti-Rabbit IgG secondary antibody for 2 h at room temperature. The slides were then dehydrated and mounted with DAPI mounting media. Images were acquired using a Leica microscope.

2.14. TUNEL Assay.

Click-iT Plus TUNEL Assay (Thermo Fisher) and an Alexa Fluor 488 dye assay kit were used in this assay to examine the fragmentation of DNA and detection of apoptosis according to the manufacturer's instructions. Shortly, a fresh frozen stomach sample was fixed in formalin and then dehydrated in increasing concentrations of alcohol. After cleaning in xylene, those tissues were submerged in paraffin. The paraffin-embedded tissues were cut to 6 μm thickness for the assay. Before conducting the assay, the section was deparaffinized with xylene by decreasing the concentration of ethanol from 100 to 70%. After deparaffinization, the stomach sections of all treatment groups were washed twice in PBS for 5 min and then incubated for 15 min with 1× Proteinase K solution (component H in the assay kit was diluted 1:25 in PBS). The slides were again fixed in 4% PFA for 20 min and washed with PBS for 5 min. To induce DNA-strand breakdown in the skin, skin samples were incubated with one unit of DNase I diluted in 1× DNase I Reaction Buffer (20 mM Tris–HCl, pH 8.4, 2 mM $MgCl_2$, 50 mM KCl) for 30 min at room temperature. After incubation, the sections were washed with DI water and 100 μL of TDT Reaction Buffer (component A in the kit) was added to each well and incubated for 10 min. The TDT reaction buffer was removed and replaced with 50 μL of the prepared TDT reaction mixture for 1 h. Next, the reaction mixture was removed, each well was rinsed with DI water, and the samples were incubated in 3% BSA and 0.1% Triton X-100 in PBS for 5 min with gentle shaking. After rinsing the slide with 1× PBS, 50 μL of freshly prepared Click-iT Plus TUNEL Reaction cocktail was added to each section for 30 min in the dark. The reaction cocktail was removed and replaced with 3% BSA in PBS for 5 min. The samples were rinsed with 1× PBS and mounted with DAPI mounting media and a coverslip and prepared for imaging by placing the tissue on a glass slide and adding a mounting medium and a coverslip. The slides were incubated for 1 h at 4 °C, and then images were taken using Leica LAS X software attached to a Leica DM2000 microscope (Leica, Germany).

2.15. Serum Biochemistry.

Serum biochemistry analysis was conducted to determine the systemic toxicity of the formulations administered to the stomach cancer mouse model. Three days after the last

dose of treatment, the mice were euthanized and 1 mL of blood was collected from the portal vein in heparin-coated tubes. Blood was centrifuged at 3000 rpm for 7 min, and plasma was collected. Serum biochemistry analysis included parameters related to liver and kidney function, e.g., aspartate aminotransferase (AST), alanine aminotransferase (ALT/GPT), alkaline phosphatase (ALP), total protein (TP), blood urea nitrogen (BUN), and creatinine (Cr). Biochemical analyses were quantified using a chemical analyzer (Element DC by Heska), and the results were presented using GraphPad Prism software.

2.16. Statistics and Image Analysis.

All experiments were carried out in triplicates, and the error bar is indicated as mean ± SD unless stated otherwise. Student *t*-test, Welch's nonparametric *t*-test, and one-way analysis of variance (ANOVA) were performed using GraphPad Prism nonlinear regression software (GraphPad Software Inc.). A *P* value of <0.05 was considered significant. * indicates statistical significance with $p < 0.05$; *** indicates statistical significance with $p < 0.001$. Image analysis of immunofluorescence and TUNEL assay was done by using the OpenCV Python programming library.

3. RESULTS AND DISCUSSION

3.1. Preparation and Characterization of BG Particles.

The barley-derived low-viscosity BG used in this study is a long-chain polysaccharide, with very low solubility in aqueous solution (Figure 1A). With gentle stirring in association with a rising temperature (up to 80 °C), the BG is dissolved completely in DI water. BG itself was used as both solubilizer and carrier of the payload for both 5FU and siRNA. The method of the formulation preparation is shown in Figure 1B. Upon heating at 80 °C, the mixture of BG forms a gel-like clear solution in the presence of water, which facilitates mixing of the hydrophobic 5FU physically. We used SEM to confirm the shape and size of the BG/5FU, BG/siRNA, and BG/5FU/siRNA formulations (Figure 1C). The SEM images of BG/5FU and BG/siRNA are provided as a supplementary information (Figure S2).

The sizes of BG, BG/5FU, BG/siRNA, and BG/5FU/siRNA were measured to be 273.66 ± 39.87, 569 ± 52.43, 470 ± 80.24, and 439.66 ± 42.33, respectively, using dynamic light scattering (DLS). The result indicates that the sizes of the 5FU- and siRNA-loaded particles were bigger compared to those of naked BG particles. The zeta potentials of BG, BG/5FU, BG/siRNA, and BG/5FU/siRNA were recorded to be 0.01 ± 0.06, 1.76 ± 0.09, −3.36 ± 0.63, and −0.91 ± 0.19, respectively. The zeta potential of BG/5FU/siRNA was increased compared to that of BG/siRNA, as BG/5FU showed a positive charge (1.76 ± 0.09 mV). The change of zeta potential confirms the successful loading of 5FU and siRNA within the BG nanoparticles. We do not see excessive changes, as the siRNA is meant to be loaded within the core and that is not expected to impact on charges on the surface.

The size and zeta potential of BG in PBS and simulated gastric juice were measured up to 5 h of incubation at room temperature. We observe that the average particle size and zeta potential changed with each loading of the compound. The average size of BG in PBS was 273 ± 39 nm in diameter at the first hour and 386 ± 54 and 583 ± 81 nm in diameter at the

third and fifth hours of incubation (Figure S1), which is an indication that the formulations tend to form aggregation and this results in an increment of the diameter. Similarly in the presence of simulated gastric juice, the average sizes of BG were found to be 276 ± 15, 399 ± 18, and 608 ± 62 nm in diameter at the first, third, and fifth hours, respectively. It is observed that with time, the size tends to increase, as well. After 5 h of incubation, the size increased by almost 200% in both saline and simulated gastric juice. As the size is almost similar in both PBS and simulated gastric juice, we can conclude that gastric juice does not impact the formulation differently than saline. BG is hydrophilic in nature, which is due to the presence of abundant hydroxyl groups that participate in hydrogen bonding with water and give the molecule the ability to hold water.[39]

The release study of 5FU was conducted in a simulated GJ. BG-incorporated 5FU shows a sustained release tendency compared to the free 5FU. The cumulative release of free 5FU reaches 100% in 5 h of dialysis, whereas for BG/5FU formulations, 100% release of 5FU takes almost 10 h, which is an indication of sustained release (Figure S3).

3.2. Mucoadhesive Properties of BG.

Figure 2A demonstrates how BG particles interact with the mucus layer within the stomach. The mucoadhesiveness and intestinal transportation of hydrophobic small molecules were further confirmed by an ex vivo diffusion study in a porcine intestine lumen. As the mucous layer is a barrier for hydrophobic molecules, to check how it crosses through the epithelial layer with assistance of BG, we used coumarin 6, a small-molecule hydrophobic fluorescent dye with similar chemical and physical properties (molecular weight and hydrophobicity) as 5FU, for ease of visualization and detection purposes.[40] Higher fluorescence intensity and accumulation of coumarin 6 were observed in the stomach layer with increment of duration of incubation. At the second hour, presence of coumarin 6 was observed within deeper layers of the intestine, which indicates the transportation of hydrophobic small molecules (Figure 2B). At the 12th hour, coumarin 6 incorporates evenly across the layers of the intestine. The same tissue was subjected to be observed under a ChemiDoc imager to capture the fluorescence signal within the cross section of the intestinal lumen, and a similar result was observed. With time (0.5, 2, and 12 h), more coumarins 6 were distributed throughout the intestine, which is an indication and confirmation of BG's ability to facilitate intestinal transportation of hydrophobic payload (Figure 2C). However, the image with only coumarin 6 shows that without BG, coumarin 6 itself is not able to diffuse through the intestinal layer.

Mucoadhesive polymers have been found to be crucial in delivering nucleic acid and peptide drugs. Recently, a study stated that the mucoadhesive nanoparticle has the potential to deliver KDM6A-mRNA on the targeted site and treat bladder cancer.[41] SPR analysis was performed to examine how BG interacts with mucin. The results demonstrate that BG has mucoadhesive properties and binds with the mucus in the presence of acid-simulated gastric juice. A carboxylated gold (Au) chip was modified with BG, and a solution of mucin was run over the chip to understand their binding kinetics, association, and dissociation profile. SPR analysis shows a response of 30,000 RU from the baseline, which confirms the strong binding affinity of BG with mucin. Curve (a) indicates the association of BG with mucin, curve (b) represents the plateau as it continues binding, and curve (c) represents the

dissociation of BG with mucin. As mucin is the main component of the mucus layer, the association and binding profile of BG with mucin provide evidence of BG's affinity with the mucus layer (Figures S3 and S4).

3.3. Stability of siRNA Payload in BG Formulation.

The stability of siRNA was measured with and without BG in PBS and simulated gastric juice. The size and zeta potential measurement of BG and BG/siRNA in the presence of PBS and simulated gastric juice were conducted from 0 to 6 h to examine the stability of siRNA payload. siRNA is a nucleic acid with a negatively charged surface and forms particles via electrostatic interaction with the partially cation-charged BG (0.0158 mV). The size of the BG/siRNA formulation was measured as 370 ± 80 nm at 0 h and 707 ± 76 nm in diameter at the sixth hour. The increasing size indicates the possibility of self-aggregation of siRNA in simulated gastric juice when attached to BG (Figure 3B,C). The result was confirmed by zeta potential analysis. As negatively charged siRNA was attached to positively charged BG, the net charge of the BG/siRNA became almost neutral. The zeta potential of BG/siRNA in simulated gastric juice was measured as −0.68 ± 0.99 mV immediately after dissolving and −0.80 ± 1.96 mV after 6 h of incubation (Figure 3E,F). The consistency of the zeta potential confirms the stability of siRNA payload within BG while being dissolved into the simulated gastric juice.

The stability of siRNA was further confirmed by agarose gel electrophoresis. The band shows that the siRNA is stable while loaded within BG for at least 8 h, both in simulated gastric juice (Figure 3D), whereas naked siRNA was found to be stable only for 2 h after incubation with GJ (Figure S4). siRNA stability analysis by NanoDrop also supports western blotting results.

3.4. In Vivo Imaging and Biodistribution.

To investigate the in vivo biodistribution and organ accumulation, coumarin 6-loaded BG was administered orally to the mice. It was examined that the BG can retain in the stomach for at least 6 h (Figure 4A). To confirm further, the ex vivo image of organs was also taken after being euthanized. In both in vivo and ex vivo imaging, BG was found to be retained only in the stomach. Except for the stomach, it went to the intestine and almost cleared out from the intestine by the sixth hour. BG retained the higher intensity of fluorescence in the stomach through the 6 h period. The result confirms that the BG is highly stomach specific, which can maintain the sustained release of hydrophobic payload (Figure 4B).

3.5. Phenotypical In Vivo Treatment Efficiency.

Stomach cancer was induced to C57BL/6 mice by feeding NMNU every other week for a 5-week period (Figure 5A). The cancer-induced mice were treated with saline, 5FU, siRNA, BG/5FU, BG/siRNA, and BG/5FU/siRNA via oral administration five times every third day. To investigate the phenotype of therapeutic progress upon treatment with formulation compared with saline-treated mice, we harvested the animal after 72 h of the fifth treatment. The size and weight of the stomach and intestine were measured immediately after the collection of the organs (Figure 5B–D). A reduction in the size and weight of the stomach was observed in the untreated and oral siRNA treatment groups, and this is an indication

of a cancerous state. However, no significant difference in the size and weight of the intestine was observed (Figure S8), which is an indication of localized cancer specific to the stomach. In stomach cancer, the mice lost appetite due to reduced production of ghrelin hormones;[42] hence, we observed a weight loss in the untreated group when compared to the healthy control. On top of that, cancer-mediated inflammation also results in the shrinkage of the organ, the stomach in this case. Reduction of size upon oral administration of nitroso compounds is one of the phenotypic indications of induction of stomach cancer, and a gain in the size back to normal, which is comparable to healthy mice, demonstrated the therapeutic efficacy of orally administered BG/siRNA/5FU formulation. The therapeutic efficacy of BG/siRNA/5FU was further confirmed with histological and immunohistochemistry analyses with the tissues.

3.6. Oral Bcl2 siRNA Causes In Vivo Gene Silencing and Apoptosis.

A TUNEL assay was conducted to investigate the apoptosis within the tissue from the stomach of healthy, untreated cancer, and treated cancer mice. We have observed significantly higher apoptosis in the stomach treated with BG/5FU/siRNA than the stomach treated with naked siRNA and both untreated and healthy control (Figure 6A,D). No fragmented DNA was observed within the stomach tissues of healthy control and untreated mice, which indicates that oral co-delivery of siRNA and 5FU induces apoptosis in stomach cancer. Apoptosis was quantified by the mean fluorescent intensity compared with healthy control and untreated control. The degree of apoptosis was calculated to be 49, 107, 38, 62, and 131% for the 5FU, BG/5FU, siRNA, BG/siRNA, and BG/5FU/siRNA groups relative to untreated control, respectively.

This reveals that apoptosis for the BG/5FU/siRNA-treated group was 69.46% more than that of BG/siRNA and 95% more than that of free siRNA. To examine if the apoptosis was caused by downregulation of Bcl2, western blotting (WB) analysis was performed from the tissue lysate of different treatment groups. The WB data shows significant downregulation of the Bcl2 gene caused by oral BG/5FU/siRNA compared to conventional naked oral siRNA (p-value <0.005) and untreated (p-value <0.0005). Data showed that the downregulation of Bcl2 gene expression was inversely proportional with the DNA fragmentation, which confirmed that the apoptosis resulted from the Bcl2 downregulation. The relative expressions of Bcl2 was 1, 1.07 ± 0.008, 1.24 ± 0.11, 0.76 ± 0.02, 0.88 ± 0.05, 1.66 ± 0.14, and 0.29 ± 0.04 for the healthy, untreated, 5FU, BG/5FU, siRNA, BG/siRNA, and BG/5FU/siRNA, respectively. This data confirms that BG-assisted orally administered siRNA was protected from the harsh gastric environment and was able to pass the mucus layer of the intestine and go into the site of action to silence the Bcl2 gene.

The stomach tissue was also utilized to analyze Bcl2 protein expression using immunohistochemistry (IHC). The anti-Bcl2-positive area was quantified in comparison to the whole tissue section stained with DAPI. The area percentage of Bcl2 antibodies for healthy, untreated, 5FU, BG/5FU, siRNA, BG/siRNA, and BG/5FU/siRNA was 1.19, 1.46, 1.22, 1.45, 0.97, 1.11, and 0.47%, respectively (Figure 7A). To measure the relative expression of Bcl2 on the tissue section, the data was calculated and compared with the stomach tissue collected from the healthy mice, where the Bcl2 expression in healthy

mice was considered as 100% (Figure 7B). The immunofluorescence data reciprocates the same as WB data. Oral delivery of BG/5FU/siRNA resulted in the lowest expression of Bcl2, as observed in WB and immunofluorescence images of tumor tissue. In the immunofluorescence image, we have observed a higher Bcl2 expression in the untreated tissue section. The untreated section had 51.20% more expression of Bcl2 compared to the healthy control. The mice treated with BG/5FU/siRNA had 111.45% ± 1.6 less expression of Bcl2 compared to untreated cancer and 68.39% less expression than mice treated with naked siRNA. Mice treated with BG/siRNA also caused less expression of Bcl2 confirmed by WB and ICH, but the combination of siRNA and 5FU resulted in a higher Bcl2 inhibition efficiency. This confirms that siRNA with 5FU produces a synergistic effect in downregulating the Bcl2 proteins.

3.7. Therapeutic Efficacy In Vivo.

A cell proliferation marker was measured by the immunofluorescence assay to evaluate the antitumor effect of the formulations. Ki67 is a protein found in the nucleus of the cancer cell. Detection of Ki67 expression has been a reliable indicator for cancer proliferation and prognosis in cancers including stomach cancer.[43] Therefore, Ki67 is considered an important indicator of therapeutic assessment and chemosensitivity. Studies show that a higher expression of Ki67 corresponds with a low chemosensitivity.[44] In this study, the stomach section from different treatment groups of mice was subjected to immunofluorescence for Ki67 protein analysis. The untreated stomach showed a higher expression of Ki67 (yellow arrow), and with treatment, specifically with BG/5FU/siRNA, the expression of Ki67 expression was reduced significantly (Figure 8A). The protein expression was quantified from immunofluorescence images. The area with Ki67-positive cells was measured compared to the whole tissue section with DAPI staining. The area (%) of healthy, untreated, 5FU, BG/5FU, siRNA, BG/siRNA, and BG/5FU/siRNA was measured as 100, 446.86, 221.44, 155.61, 498.85, 278.82, and 90.27%, respectively. The Ki67 expression in the untreated group was 346.86% higher in the untreated group compared to the healthy control, whereas, with the BG/5FU/siRNA treatment group, the expression was reduced by 356.59% when compared to the stomach of untreated cancer mice (Figure 8B). We have also observed a partial expression of Ki67 to the group of mice treated with 5FU, which is comparatively higher than in mice treated with BG/5FU/siRNA.[45]

H&E staining with stomach tissue was conducted to measure the anticancer therapeutic effect of stomach cancer as well as the inflammatory effect among the tissues/cells around the cancer. Figure 9 represents the H&E staining image of the same stomach section in different magnifications. To visualize the whole tumor area, the image was taken at 10× magnification, and to understand the pathophysiology, a higher-magnification image was taken at 40× by a slide scanner. As seen in Figure 9, the presence of tumors in the stomach is indicated by the black arrow. Moreover, a large intramucosal tumor was observed in the stomach of untreated cancer mice and cancer mice treated with siRNA and BG/siRNA. However, no visible tumor was observed in the stomach of the cancer mice treated with BG/5FU/siRNA. The total remission of cancer indicates the ability and anticancer efficacy of oral delivery of 5FU/siRNA assisted by BG.

In Figure 8B, the images were taken at 40× and then the red rectangular area was cropped to magnify for better and clearer visualization of the tissue morphology. The higher magnification of the images shows adenocarcinoma in the untreated group where there was higher staining of nuclei, irregular glandular space, and distortion of the normal epithelial structure.[46] A signet ring cell was also found in the untreated stomach cancer tissue. No improvement of tumor was observed in the naked siRNA-treated stomach section. However, mice treated with BG/5FU/siRNA and BG/5FU demonstrated that the cellular structure almost resembled a healthy stomach.

3.8. Serum Biochemistry and Toxicity.

To examine the systemic side effect mediated by the treatment modalities, serum analysis was conducted with the blood collected from healthy control, untreated, and treatment groups. Liver and kidney toxicity was measured by quantifying the presence of total protein (TP), alanine aminotransferase (ALT), creatinine, and blood urea nitrogen (BUN) in blood compared with healthy control. As depicted in Figure 10, none of the parameters were found out of the reference range, which confirms that the oral formulations are not significantly toxic to the liver and kidney. As the treatments were given orally, the H&E staining of the small intestine was also done and no toxicity was observed in the histological section of the duodenum, jejunum, and ilium of the different treatment groups (Figure S9).

4. CONCLUSIONS

Stomach-specific oral delivery of anticancer therapeutics can enhance the retention duration of the therapeutic modalities, thus improving the therapeutic effect by increasing the drug concentration within the site of cancer. 5FU is the first-line treatment of choice for stomach cancer; however, toxic effect and development of resistance are the major concern. Considering the risk-to-benefit ratio of using 5FU, there is a concern about their broad-spectrum application for various cancers. In this study, oral delivery of 5FU and Bcl2 siRNA was used to enhance the therapeutic effect by the synergistic effect of 5FU and siRNA. RNAi is gaining popularity as an anticancer treatment option because of selective gene silencing and no off-targeting effect, which provides better therapeutic efficacy and fewer side effects. To overcome the challenges associated with the oral delivery of siRNA, we have developed a nanocarrier composed of BG, a highly biocompatible polysaccharide. The BG not only protects the payload of siRNA to maintain their stability but also enhances their retention within the stomach for at least 6 h. The co-delivery of BG/5FU/siRNA was shown to downregulate Bcl2 expression and apoptosis of cancer cells. The TUNEL assay confirms the apoptosis of tumor cells. The Ki67 marker was also reduced with the treatment, and histological staining shows almost complete remission of the tumor region with BG/5FU/siRNA formulation. Our findings demonstrate that this oral therapeutic modality has potential for treating stomach cancer and the co-delivery of siRNA and 5FU is more effective than individual entities such as free siRNA and 5FU. However, the pathway of producing a synergistic effect in silencing Bcl2 has not been examined in this study. Therefore, we aim to continue this study to understand the mechanism of action of 5FU and Bcl2 siRNA combination.

Supplementary Material

Refer to Web version on PubMed Central for supplementary material.

ACKNOWLEDGMENTS

We acknowledge funding by the Cancer Prevention Research Institute of Texas (CPRIT) through a Texas Regional Excellence in Cancer Award (TREC) under Award No. PR210153, and the National Institutes of Health (NIH) under Award No. R03OD032624. The contents of this paper are solely the authors' responsibility and do not necessarily represent the official views of NIH. Contents for graphics and cartoons including table of contents were obtained from smart.servier.com and Microsoft PowerPoint.

REFERENCES

(1). Rawla P; Barsouk A Epidemiology of Gastric Cancer: Global Trends, Risk Factors and Prevention. Gastroenterol. Rev 2019, 14, 26–38.

(2). Thrift AP; El-Serag HB Burden of Gastric Cancer. Clin. Gastroenterol. Hepatol 2020, 18, 534–542. [PubMed: 31362118]

(3). Drugs Approved for Stomach (Gastric) Cancer - NCI. https://www.cancer.gov/about-cancer/treatment/drugs/stomach (accessed 2023-01-05).

(4). Zhang C; Liu Z-K Gene Therapy for Gastric Cancer: A Review. World J. Gastroenterol 2003, 9, 2390. [PubMed: 14606062]

(5). Wang LJ; Jin HC; Wang X; Lam EKY; Zhang JB; Liu X; Chan FKL; Si JM; Sung JJY ZIC1 Is Downregulated through Promoter Hypermethylation in Gastric Cancer. Biochem. Biophys. Res. Commun 2009, 379, 959–963. [PubMed: 19135984]

(6). Zhang N; Wang A-Y; Wang X-K; Sun X-M; Xue H-Z GAS5 Is Downregulated in Gastric Cancer Cells by Promoter Hypermethylation and Regulates Adriamycin Sensitivity. Eur. Rev. Med. Pharmacol. Sci 2016, 20, 3199–3205. [PubMed: 27466992]

(7). Chen H; Pan Y; Cheng Z-Y; Wang Z; Liu Y; Zhao Z-J; Fan H Hypermethylation and Clinicopathological Significance of RASAL1 Gene in Gastric Cancer. Asian Pac. J. Cancer Prev 2013, 14, 6261–6265. [PubMed: 24377515]

(8). Eftang LL; Esbensen Y; Tannæs TM; Blom GP; Bukholm IR; Bukholm G Up-Regulation of CLDN1 in Gastric Cancer Is Correlated with Reduced Survival. BMC Cancer 2013, 13, 586. [PubMed: 24321518]

(9). Delario AJ Problems in the Diagnosis of Cancer of the Stomach. Am. J. Cancer 1936, 27, 334–340.

(10). Gu E; Song W; Liu A; Wang H SCDb: An Integrated Database of Stomach Cancer. BMC Cancer 2020, 20, 490. [PubMed: 32487193]

(11). Galia E; Nicolaides E; Hörter D; Löbenberg R; Reppas C; Dressman JB Evaluation of Various Dissolution Media for Predicting In Vivo Performance of Class I and II Drugs. Pharm. Res 1998, 15, 698–705. [PubMed: 9619777]

(12). Rajput GC; Majmudar FD; Patel JK; Patel KN; Thakor RS; Patel BP; Rajgor NB Stomach Specific Mucoadhesive Tablets as Controlled Drug Delivery System–A Review Work. Int. J. Pharm. Biol. Res 2010, 1, 30–41.

(13). Alshaer W; Zureigat H; Al Karaki A; Al-Kadash A; Gharaibeh L; Hatmal MM; Aljabali AAA; Awidi A SiRNA: Mechanism of Action, Challenges, and Therapeutic Approaches. Eur. J. Pharmacol 2021, 905, No. 174178. [PubMed: 34044011]

(14). Islam T; Huda MN; Ahsan MA; Afrin H; Joseph J Salazar C; Nurunnabi M Theoretical and Experimental Insights into the Possible Interfacial Interactions between β-Glucan and Fat Molecules in Aqueous Media. J. Phys. Chem. B 2021, 125, 13730–13743. [PubMed: 34902976]

(15). Vetvicka V; Vannucci L; Sima P B-glucan as a New Tool in Vaccine Development. Scand. J. Immunol 2020, 91, No. e12833. [PubMed: 31544248]

(16). Lee D-Y; Nurunnabi M; Kang SH; Nafiujjaman M; Huh KM; Lee Y; Kim Y-C Oral Gavage Delivery of PR8 Antigen with β-Glucan-Conjugated GRGDS Carrier to Enhance M-Cell

Targeting Ability and Induce Immunity. Biomacromolecules 2017, 18, 1172–1179. [PubMed: 28278374]

(17). Chowdhury AS; Geetha Bai R; Islam T; Abir M; Narayan M; Khatun Z; Nurunnabi M Bile Acid Linked β-Glucan Nanoparticles for Liver Specific Oral Delivery of Biologics. Biomater. Sci 2022, 10, 2929–2939. [PubMed: 35471198]

(18). Ciecierska A; Drywien M; Hamulka J; Sadkowski T Nutraceutical Functions of Beta-Glucans in Human Nutrition. Roczniki Państwowego Zakładu Higieny 2019, 315–324. [PubMed: 31960663]

(19). Schwartz B; Hadar Y Possible Mechanisms of Action of Mushroom-Derived Glucans on Inflammatory Bowel Disease and Associated Cancer. Ann. Transl. Med 2014, 2, 19. [PubMed: 25332995]

(20). Su Y; Chen L; Yang F; Cheung PCK Beta-d-Glucan-Based Drug Delivery System and Its Potential Application in Targeting Tumor Associated Macrophages. Carbohydr. Polym 2021, 253, No. 117258. [PubMed: 33278940]

(21). Esquivel SV; Bhatt HN; Diwan R; Habib A; Lee W-Y; Khatun Z; Nurunnabi M β-Glucan and Fatty Acid Based Mucoadhesive Carrier for Gastrointestinal Tract Specific Local and Sustained Drug Delivery. Biomolecules 2023, 13, 768. [PubMed: 37238639]

(22). Xu Z-Y; Tang J-N; Xie H-X; Du Y-A; Huang L; Yu P-F; Cheng X-D 5-Fluorouracil Chemotherapy of Gastric Cancer Generates Residual Cells with Properties of Cancer Stem Cells. Int. J. Biol. Sci 2015, 11, 284–294. [PubMed: 25678847]

(23). Kohnoe S; Maehara Y; Takahashi I; Emi Y; Baba H; Sugimachi K Treatment of Advanced Gastric Cancer with 5-Fluorouracil and Cisplatin in Combination with Dipyridamole. Int. J. Oncol 1998, 1203. [PubMed: 9824632]

(24). Japanese Gastric Cancer Association. Japanese Gastric Cancer Treatment Guidelines 2010 (Ver. 3). Gastric Cancer 2011, 14, 113–123. [PubMed: 21573742]

(25). Abdel-Rahman O 5-Fluorouracil-Related Cardiotoxicity; Findings From Five Randomized Studies of 5-Fluorouracil-Based Regimens in Metastatic Colorectal Cancer. Clin. Colorectal Cancer 2019, 18, 58–63. [PubMed: 30470591]

(26). Peng H; Yang H; Song L; Zhou Z; Sun J; Du Y; Lu K; Li T; Yin A; Xu J; Wei S Sustained Delivery of SiRNA/PEI Complex from in Situ Forming Hydrogels Potently Inhibits the Proliferation of Gastric Cancer. J. Exp. Clin. Cancer Res 2016, 35, 57. [PubMed: 27029190]

(27). Afrin H; Geetha Bai R; Kumar R; Ahmad SS; Agarwal SK; Nurunnabi M Oral Delivery of RNAi for Cancer Therapy. Cancer Metastasis Rev. 2023, 1. [PubMed: 36917329]

(28). Song C; Han Y; Luo H; Qin Z; Chen Z; Liu Y; Lu S; Sun H; Zhou C HOXA10 Induces BCL2 Expression, Inhibits Apoptosis, and Promotes Cell Proliferation in Gastric Cancer. Cancer Med. 2019, 8, 5651–5661. [PubMed: 31364281]

(29). Siddiqui WA; Ahad A; Ahsan H The Mystery of BCL2 Family: Bcl-2 Proteins and Apoptosis: An Update. Arch. Toxicol 2015, 89, 289–317. [PubMed: 25618543]

(30). Bold RJ; Virudachalam S; McConkey DJ BCL2 Expression Correlates with Metastatic Potential in Pancreatic Cancer Cell Lines. Cancer 2001, 92, 1122–1129. [PubMed: 11571724]

(31). Boidol B; Kornauth C; van der Kouwe E; Prutsch N; Kazianka L; Gültekin S; Hoermann G; Mayerhoefer ME; Hopfinger G; Hauswirth A; Panny M; Aretin M-B; Hilgarth B; Sperr WR; Valent P; Simonitsch-Klupp I; Moriggl R; Merkel O; Kenner L; Jäger U; Kubicek S; Staber PB First-in-Human Response of BCL-2 Inhibitor Venetoclax in T-Cell Prolymphocytic Leukemia. Blood 2017, 130, 2499–2503. [PubMed: 28972014]

(32). Mei J; Liu G; Li R; Xiao P; Yang D; Bai H; Hao Y LncRNA SNHG6 Knockdown Inhibits Cisplatin Resistance and Progression of Gastric Cancer through MiR-1297/BCL-2 Axis. Biosci. Rep 2021, 41, BSR20211885.

(33). Kang SH; Revuri V; Lee SJ; Cho S; Park IK; Cho KJ; Bae WK; Lee YK Oral SiRNA Delivery to Treat Colorectal Liver Metastases. ACS Nano 2017, 10417. [PubMed: 28902489]

(34). Muddineti OS; Rompicharla SVK; Kumari P; Bhatt H; Ghosh B; Biswas S Vitamin-E/Lipid Based PEGylated Polymeric Micellar Doxorubicin to Sensitize Doxorubicin-Resistant Cells towards Treatment. React. Funct. Polym 2019, 134, 49–57.

(35). Afrin H; Huda MN; Islam T; Oropeza BP; Alvidrez E; Abir MI; Boland T; Turbay D; Nurunnabi M Detection of Anticancer Drug-Induced Cardiotoxicity Using VCAM1-Targeted Nanoprobes. ACS Appl. Mater. Interfaces 2022, 37566. [PubMed: 35939041]

(36). Yamachika T; Nakanishi H; Inada K; Tsukamoto T; Shimizu N; Kobayashi K; Fukushima S; Tatematsu M N-Methyl-N-Nitrosourea Concentration-Dependent, Rather than Total Intake-Dependent, Induction of Adenocarcinomas in the Glandular Stomach of BALB/c Mice. Jpn. J. Cancer Res 1998, 89, 385–391. [PubMed: 9617343]

(37). Hayakawa Y; Fox JG; Gonda T; Worthley DL; Muthupalani S; Wang TC Mouse Models of Gastric Cancer. Cancers 2013, 5, 92. [PubMed: 24216700]

(38). Boegh M; Nielsen HM Mucus as a Barrier to Drug Delivery – Understanding and Mimicking the Barrier Properties. Basic Clin. Pharmacol. Toxicol 2015, 116, 179–186. [PubMed: 25349046]

(39). Kaur R; Sharma M; Ji D; Xu M; Agyei D Structural Features, Modification, and Functionalities of Beta-Glucan. Fibers 2020, 1.

(40). Miao X; Li Y; Wyman I; Lee SMY; Macartney DH; Zheng Y; Wang R Enhanced in Vitro and in Vivo Uptake of a Hydrophobic Model Drug Coumarin-6 in the Presence of Cucurbit[7]Uril. MedChemComm 2015, 6, 1370–1374.

(41). Kong N; Zhang R; Wu G; Sui X; Wang J; Kim NY; Blake S; De D; Xie T; Cao Y; Tao W Intravesical Delivery of KDM6A-MRNA via Mucoadhesive Nanoparticles Inhibits the Metastasis of Bladder Cancer. Proc. Natl. Acad. Sci 2022, 119, No. e2112696119. [PubMed: 35131941]

(42). Aydin S; Ozercan İH; Dagli F; Aydin S; Dogru O; Celebi S; Akin O; Guzel SP Ghrelin Immunohistochemistry of Gastric Adenocarcinoma and Mucoepidermoid Carcinoma of Salivary Gland. Biotech. Histochem 2005, 80, 163–168. [PubMed: 16298902]

(43). Lazăr D; Tăban S; Sporea I; Dema A; Cornianu M; Lazăr E; Goldiş A; Vernic C Ki-67 Expression in Gastric Cancer. Results from a Prospective Study with Long-Term Follow-Up. Rom. J. Morphol. Embryol 2010, 51, 655–661. [PubMed: 21103622]

(44). Itaya M; Yoshimoto J; Kojima K; Futagawa S Usefulness of P53 Protein, Bcl-2 Protein and Ki-67 as Predictors of Chemosensitivity of Malignant Tumors. Oncol. Rep 1999, 675. [PubMed: 10203614]

(45). Sethy C; Kundu CN 5-Fluorouracil (5-FU) Resistance and the New Strategy to Enhance the Sensitivity against Cancer: Implication of DNA Repair Inhibition. Biomed. Pharmacother 2021, 137, No. 111285. [PubMed: 33485118]

(46). Tsurudome I; Miyahara R; Funasaka K; Furukawa K; Matsushita M; Yamamura T; Ishikawa T; Ohno E; Nakamura M; Kawashima H; Watanabe O; Nakaguro M; Satou A; Hirooka Y; Goto H In Vivo Histological Diagnosis for Gastric Cancer Using Endocytoscopy. World J. Gastroenterol 2017, 23, 6894–6901. [PubMed: 29085232]

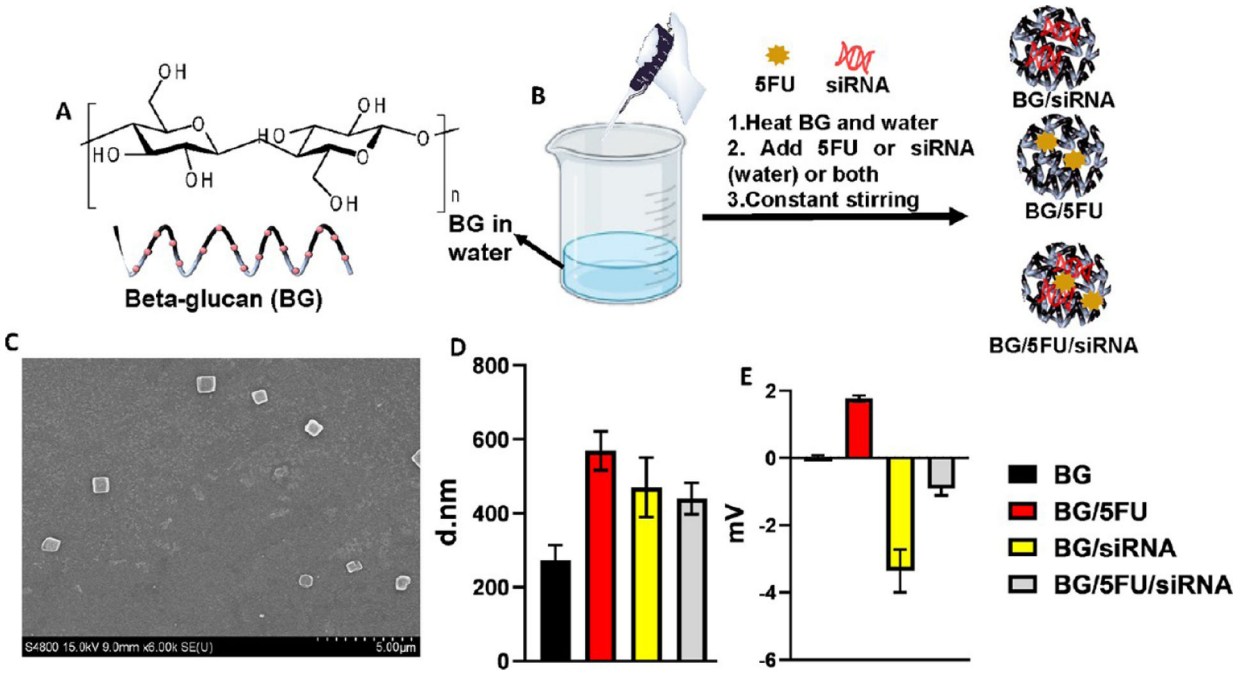

Figure 1.

Chemical and physical properties of the formulations. (A) Chemical structure (repeating unit) and schematic presentation of BG. (B) Schematic representation of preparation of formulations; BG/siRNA, BG/5FU, and BG/5FU/siRNA. (C) SEM images of BG/5FU/siRNA BG showed a smooth surface and nano size (scale bar = 5 μm). (D) Size distribution and (E) zeta potential of all the formulations measured using a DLS and a zeta analyzer, respectively. Data presented as mean ± SEM, where $n = 3$.

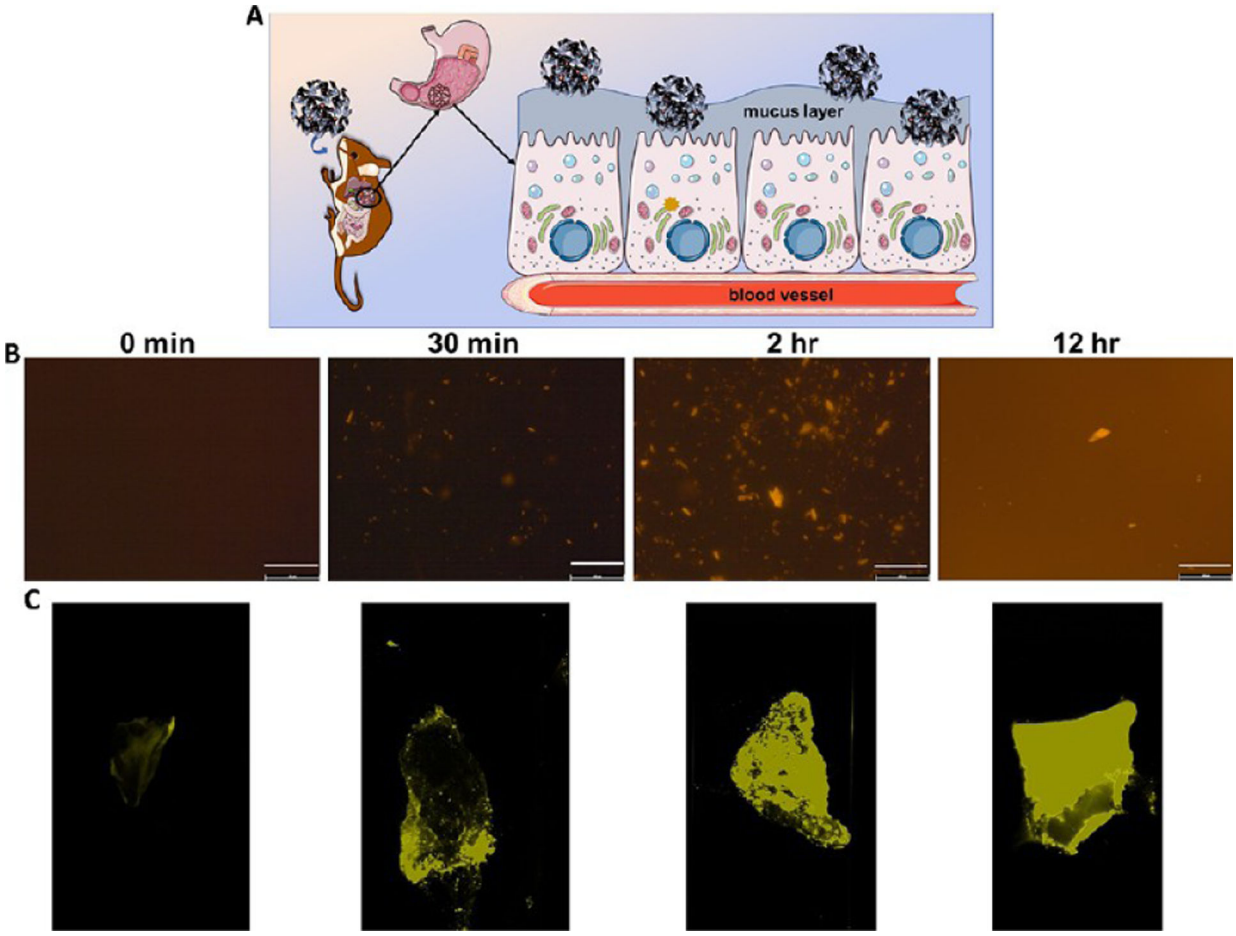

Figure 2.

Mucoadhesive properties of BG. (A) A schematic representation of mucoadhesiveness of BG and how it facilitates the transport of siRNA and 5FU across the epithelium. BG/coumarin 6 was incubated on the porcine intestine for a different period and washed for 5 min before taking the image. (B) Images show that BG facilitates to penetrate hydrophobic coumarin 6 into the intestinal layer with time, whereas only coumarin 6 without BG does not diffuse through the intestine. (C) The same section of BG/coumarin 6 was taken under a ChemiDoc Imager (Bio-Rad, USA), and the result corresponded with the image of BG/coumarin 6 in (B). The components in (A) were obtained from smart.servier.com.

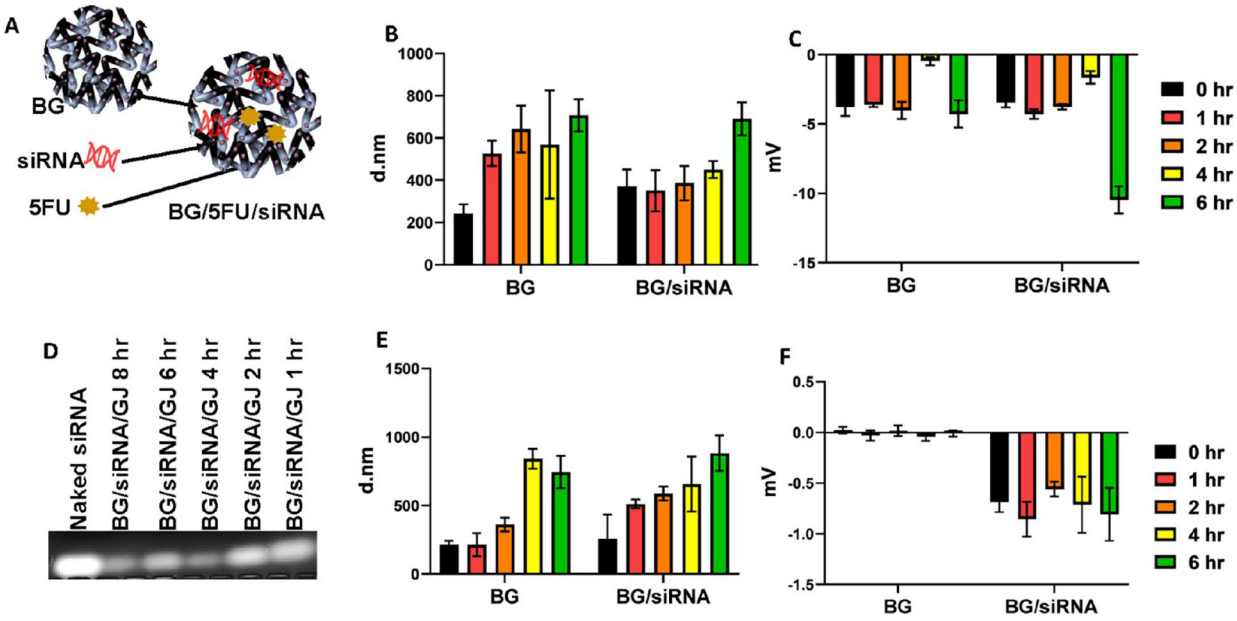

Figure 3.

Stability of BG/siRNA particles in PBS and simulated gastric juice. Schematic of the formulation (A). The size and zeta potential of BG and BG/siRNA in PBS and gastric juice were measured. Particle size distribution of BG and BG/siRNA was observed in PBS (B) and in simulated gastric juice (C) at 0, 1, 2, 4, and 6 h. It was observed that after adding siRNA, the size of BG increased initially at 0 h of measurement. (D) Gel electrophoresis analysis of naked siRNA and BG/siRNA incubated with simulated gastric juice up to 6 h. The image shows that naked siRNA was not stable in simulated gastric juice even 1 h after mixing whereas BG/siRNA was found to be stable up to 6 h after mixing with simulated gastric juice. The zeta potential of BG and siRNA with BG was also observed in PBS (E) and in simulated gastric juice (F). The zeta potential of siRNA with BG showed a negative charge constantly up to 6 h. Data presented as mean ± SEM, where $n = 3$.

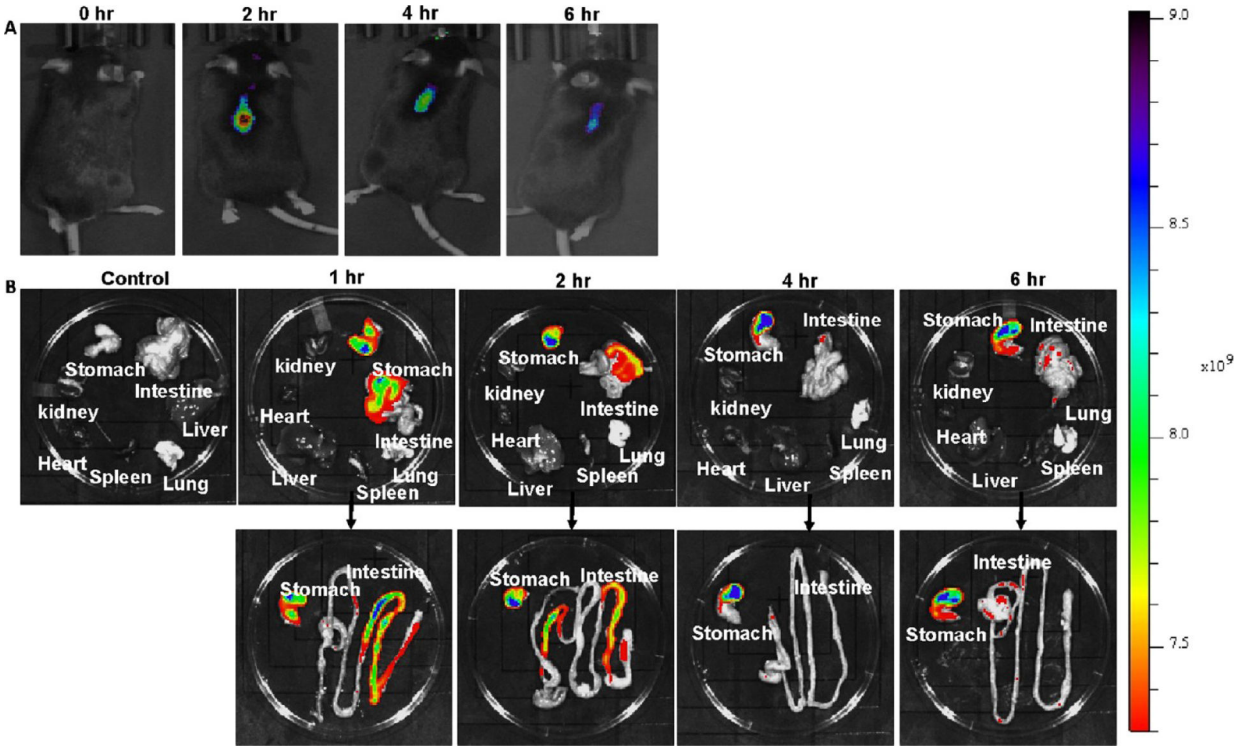

Figure 4.

Fluorescence imaging to investigate biodistribution. (A) In vivo imaging shows noninvasive fluorescence-based localization of orally administered formulations. (B) Ex vivo images of the harvested organs show biodistribution of mice at pre-administration and after 2, 4, and 6 h. Magnified images of the GI tract show that BG particles remain in the stomach at least for 6 h whereas they slowly diffused via the intestine.

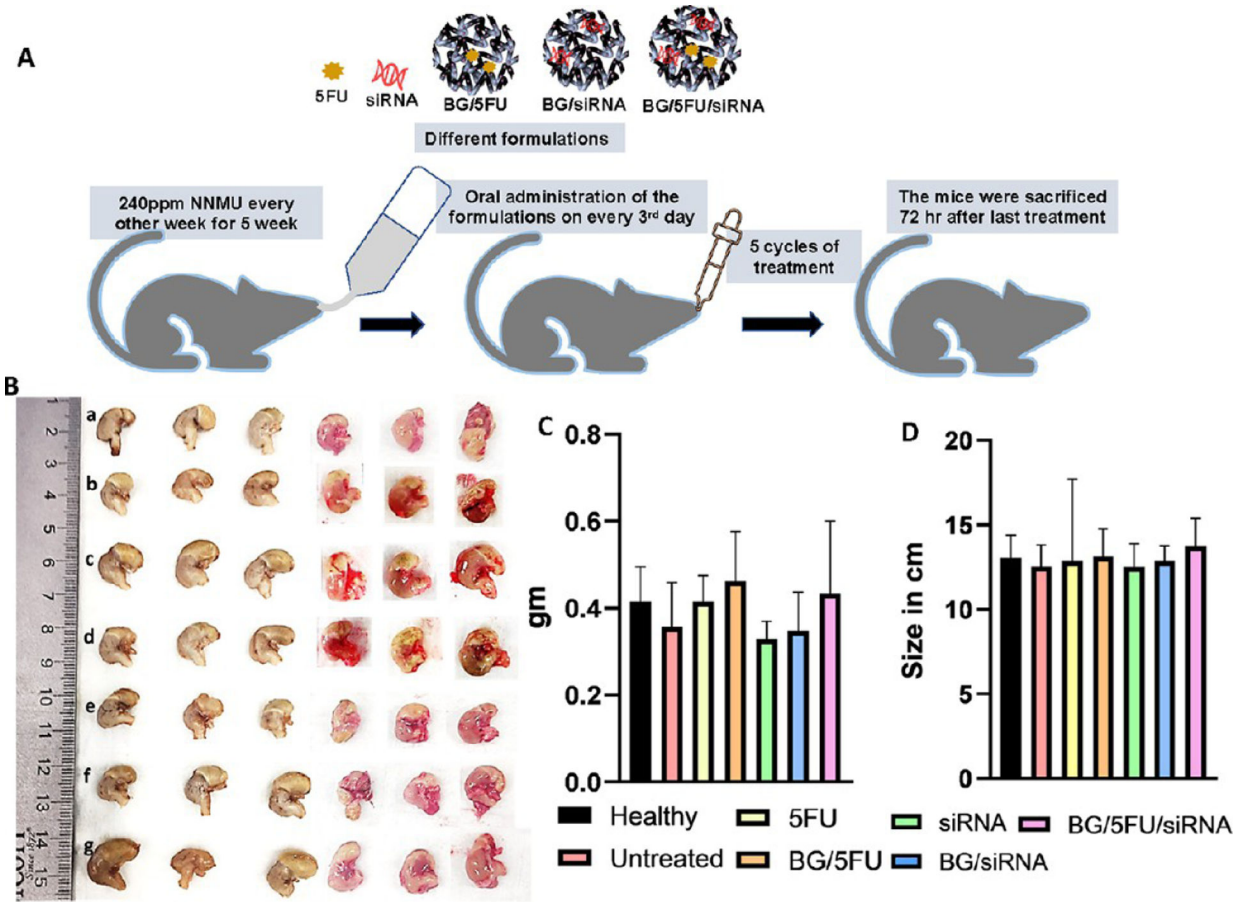

Figure 5.

In vivo therapeutic efficacy. (A) Schematic of animal model preparation and treatment. (B) Image of the stomach collected from different groups of treatment—healthy (a), untreated cancer (c), BG/5FU (c), 5FU (d), siRNA (e), BG/siRNA (f), and BG/5FU/siRNA (g). (C, D) Weight and size of the stomach. Data presented as mean ± SEM, where $n = 5$.

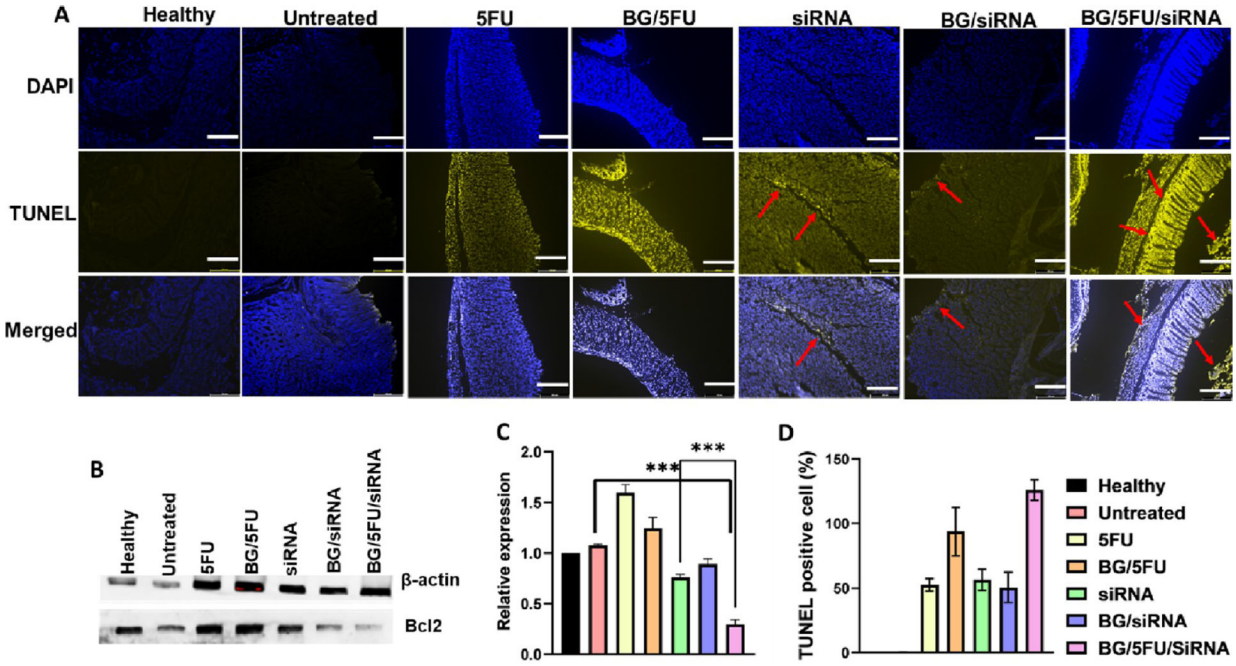

Figure 6.

Immunohistochemistry to attribute apoptosis. (A) TUNEL assay shows broken nucleus (red arrow) in siRNA, BG/siRNA, and BG/5FU/siRNA groups. Scale bars represent 200 μm. (B) Western blot analysis also shows reduced Bcl2 expression in the BG/5FU/siRNA group compared to naked siRNA and BG/siRNA. The error bar represents the standard deviation. (C) Quantitative analysis of WB. (D) Apoptosis in percentage. Data presented as mean ± SEM, where $n = 5$. P value <0.0001 is denoted as ***.

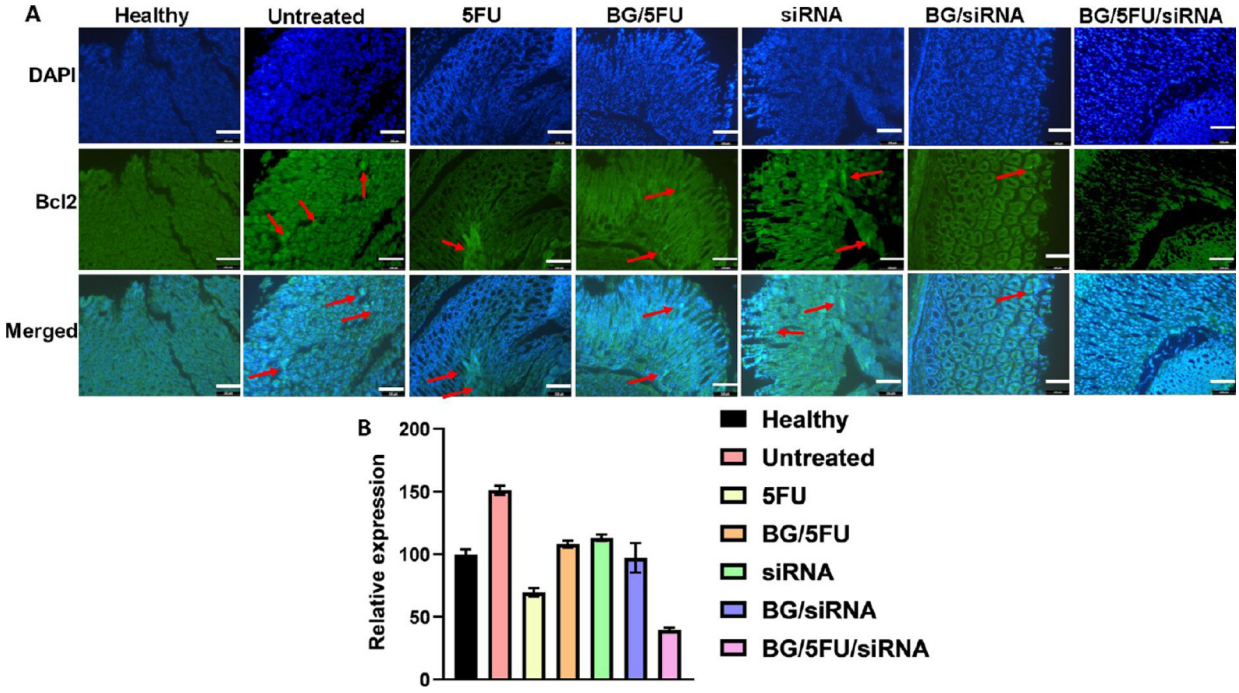

Figure 7.

Immunohistochemistry to attribute the expression of Bcl2 proteins. (A) Immunohistochemistry for Bcl-2 proteins shows a higher expression of Bcl-2 in untreated mice stomachs (red arrow). The naked oral siRNA treatment group also had more Bcl-2 expression than BG/siRNA and BG/5FU/siRNA. The scale bar represents 100 μm. (B) Quantification of Bcl2 immunofluorescence data analysis was presented. Data presented as mean ± SEM, where $n = 5$.

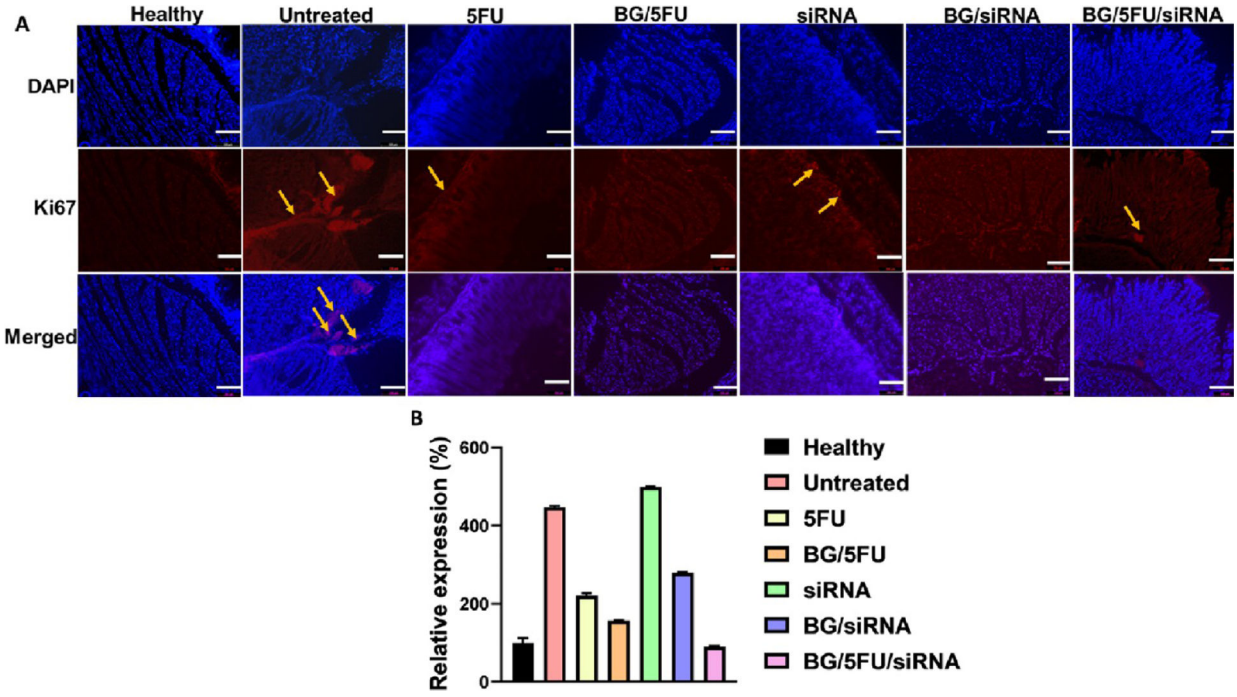

Figure 8.

Immunofluorescence for Ki67 of stomach sections of different treatment groups. (A) A higher expression of Ki67 (yellow arrow) was observed in the untreated group, whereas after treatment, the expression got reduced specially with BG/5FU/siRNA formulation. Scale bar represents 100 μm. (B) Ki67 expression was quantified compared to healthy control. Data presented as mean ± SEM, where $n = 5$.

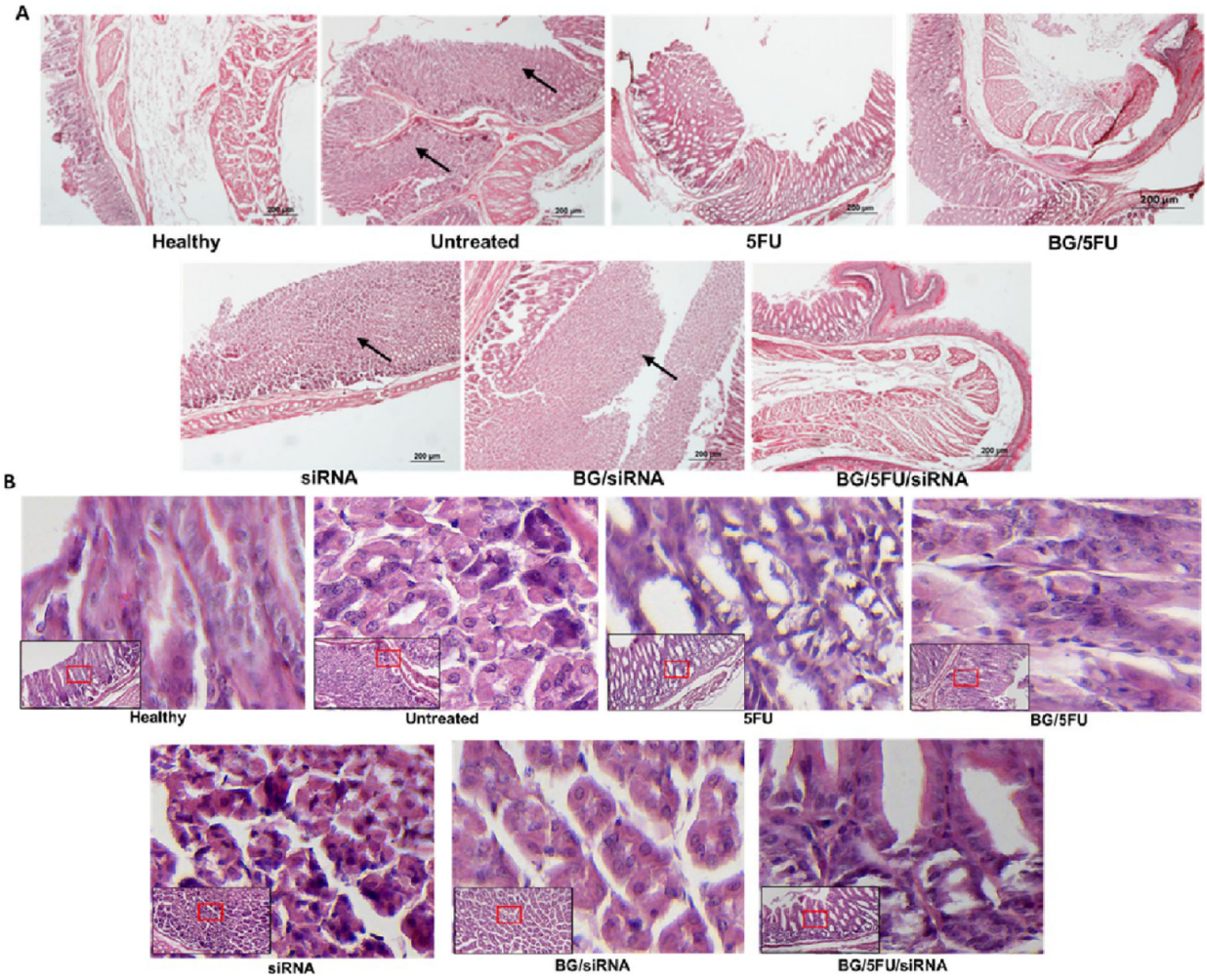

Figure 9.

Histology of stomach. (A) The histological staining (H&E) shows a growth (blue arrow) in the untreated section, while after treatment with 5FU, 5FU/BG, and BG/5FU/siRNA, the tumor region got significantly reduced. (B) H&E staining of stomach cancer sections with 40× magnification. The red rectangular area was cropped and magnified for better morphological understanding. The untreated, naked siRNA, and BG/siRNA show the feature of adenocarcinoma. The section of the BG/5FU/siRNA treatment group almost resembles a healthy stomach.

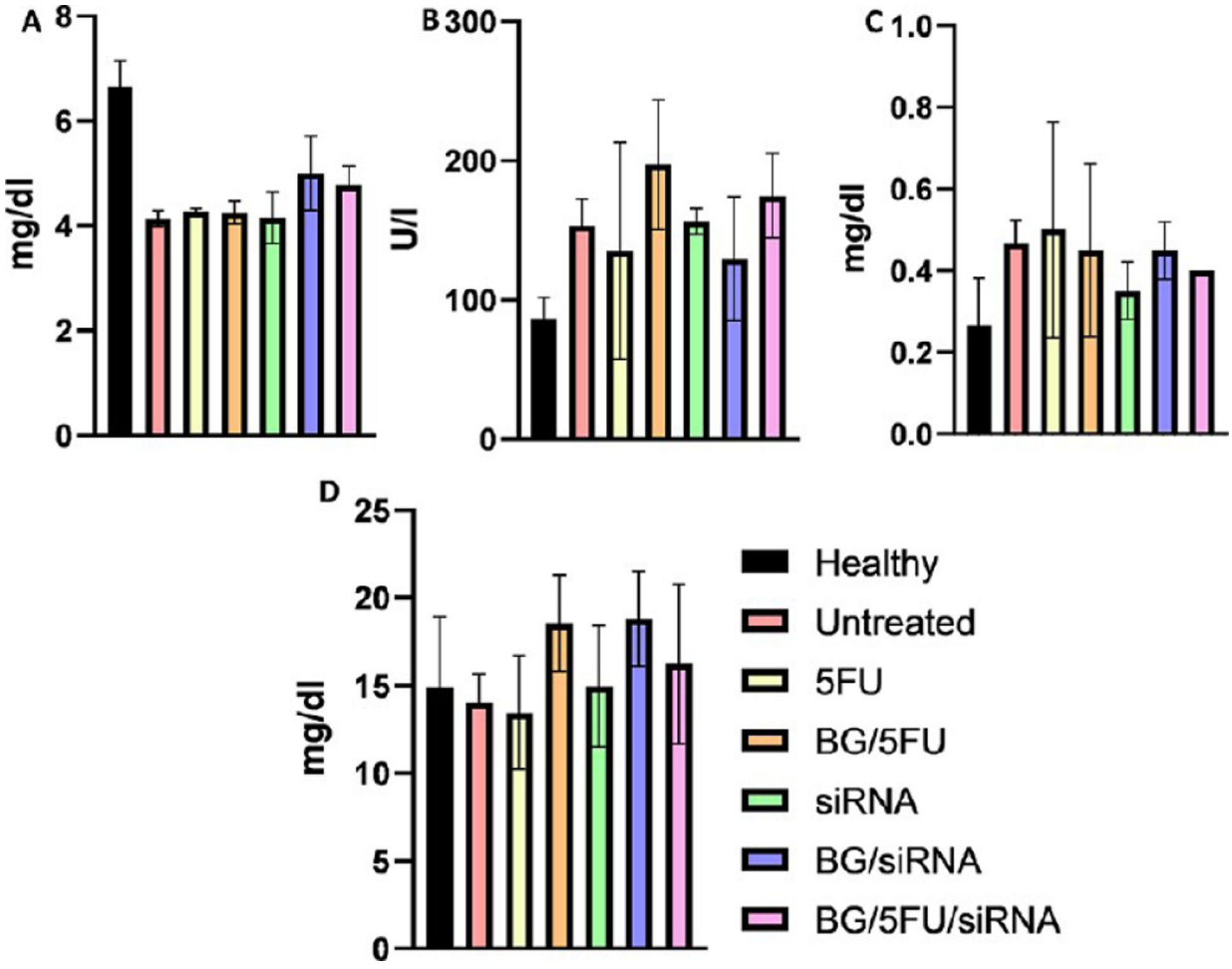

Figure 10.

Serum biochemistry to demonstrate toxicity. Serum analysis for (A) total protein (TP), (B) alanine aminotransferase (ALT), (C) creatinine, and (D) blood urea nitrogen (BUN) does not show any significant difference of the treatment group with the untreated. Data presented as mean ± SEM, where $n = 5$.

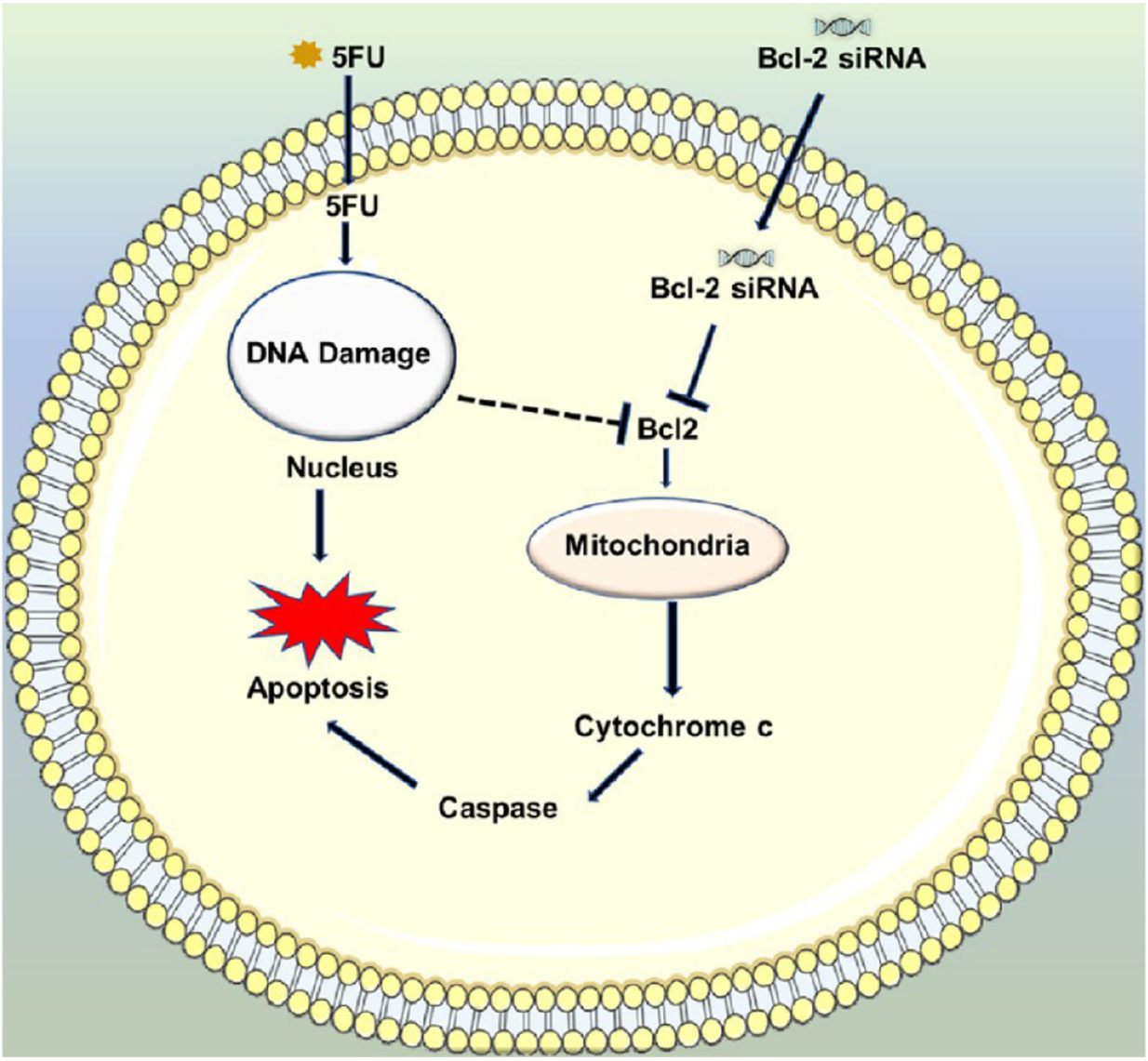

Scheme 1. The Mechanism of Action of Co-Treatment of 5-FU and Bcl2 siRNA and Their Synergy to Improve Stomach Cancer Treatment[a]

[a]The components of this scheme were obtained from smart.servier.com.